

RESEARCH ARTICLE

10.1002/2015JE004877

Key Points:

- Impactors with geologically short return times are capable of puncturing Europa's ice
- Penetration sites may form conduits from the surface to the underlying ocean

Supporting Information:

- Table S1, Table S2 caption, and Movies S1–S4 captions
- Movie S1
- Movie S2
- Movie S3
- Movie S4

Correspondence to:

R. Cox,
rcox@williams.edu

Citation:

Cox, R., and A. W. Bauer (2015), Impact breaching of Europa's ice: Constraints from numerical modeling, *J. Geophys. Res. Planets*, 120, 1708–1719, doi:10.1002/2015JE004877.

Received 19 JUN 2015

Accepted 18 SEP 2015

Accepted article online 14 OCT 2015

Published online 27 OCT 2015

Impact breaching of Europa's ice: Constraints from numerical modeling

Rónadh Cox¹ and Aaron W. Bauer¹

¹Geosciences Department, Williams College, Williamstown, Massachusetts, USA

Abstract Numerical simulations show that impactors can penetrate Europa's ice, creating conduits to the underlying ocean. Breaching becomes inevitable when transient cavity depth exceeds 90% of ice thickness. Results indicate that a 0.5 km comet would penetrate 5 km ice, and a 5 km comet could breach 40 km ice. Thinner ice would be breached more frequently, thicker ice less so, but even the 40 km upper estimates for ice thickness would be penetrated by comets with recurrence intervals less than 250 Ma. If actual ice thickness is 8–13 km (indicated by comparing European and simulated crater geometries), the ocean could be exposed by impactors in the range 0.7–1.5 km, which have recurrence intervals \approx 3 to 7 Ma. Thus, it seems that Europa's ice has been penetrated often in the past and possibly in geologically recent time. The largest known impact sites, Callanish and Tyre, probably represent transition from craters to penetrating impacts. The geomorphic expression of full penetration must exist on the surface; chaos terrain is a candidate. Astrobiological materials could be transported to the ocean via these impact-created conduits.

1. Introduction

How does Europa's sub-ice ocean communicate with the surface? And how thick is the ice barrier? These questions have been at the forefront of Europa studies since *Galileo* data revealed the probable existence of a liquid water layer [Kivelson *et al.*, 2000]. The presence of salts in surface ice [e.g., Hand and Carlson, 2015] indicates transfer of ocean materials to the exterior, but how that happens is not understood, nor do we know how materials might move from the surface into the ocean beneath. This latter is particularly relevant to exobiological modeling: organic molecules have certainly been delivered by impacting comets, and radiative bombardment within Jupiter's magnetosphere produces oxidants and organic molecules at Europa's surface; but transport to the ocean is required to provide an inventory of biologic precursors and energy sources to Europa's putative biotic system [Chyba and Phillips, 2001].

Impacts have the potential to excavate through the ice and create surface-to-ocean conduits via which two-way mass transfer might be achieved [Turtle and Pierazzo, 2001; Turtle and Ivanov, 2002; Senft and Stewart, 2011; Bray *et al.*, 2014], but whether this is an important process on Europa—or whether it occurs at all—has not been established. In this study we model the limiting conditions for ice penetration and define a set of breaching criteria. Using impactor population statistics [Zahnle *et al.*, 1998, 2003], we estimate likely recurrence intervals for crust-breaching impactors and show that breaching must be a recurring event at Europa. By comparing the geometry of numerically simulated craters with measurements from Europa, we test existing estimates for ice thickness [Schenk, 2002; Bray *et al.*, 2014] and confirm that it is likely to be close to 10 km. But we also show that—no matter what ice thickness is preferred for Europa—there is an impactor size with geologically reasonable recurrence interval that is likely to breach it. And thus, it is plausible that impacts may mediate transfer of prebiotic components to the ocean.

2. Numerical Modeling Methods

Simulating planetary impact dynamics, because of the high shocks and strain rates involved, requires code that can solve equations for conservation of momentum, mass, and energy simultaneously with the equation(s) of state and constitutive relationships (that describe the material response). These shock physics codes can predict impactor and target responses from first principles and are therefore a standard mechanism for investigating the dynamics and outcomes of impacts on Earth and elsewhere [e.g., Turtle and Pierazzo, 2001; Weiss *et al.*, 2006; Wünnemann *et al.*, 2006; Bray *et al.*, 2008; Pierazzo *et al.*, 2008; Senft and Stewart, 2011; Jutzi *et al.*, 2015].

We used the iSALE (impact Simplified Arbitrary Lagrangian Eulerian) code v.7.0, which was developed from earlier SALE code [Amdsen *et al.*, 1980] specifically for impact simulations [Collins *et al.*, 2004, 2011]. All impacts were vertical (required by the axisymmetric structure of the 2-D code). The modeled target consisted of a solid ice sheet overlying liquid water that extended to the base of the computational mesh. The range of ice thicknesses, 1–40 km, corresponds to the published range of estimates for Europa [e.g., Schenk, 2002; Billings and Kattenhorn, 2005; Nimmo and Giese, 2005; Singer *et al.*, 2010]. Our constitutive model for ice (Table S1 in the supporting information) was based on recent work [Senft and Stewart, 2011; Bray *et al.*, 2014], and we used the Tillotson equation of state as implemented in iSALE [Wünnemann *et al.*, 2006]. For the underlying water, we experimented with both Tillotson and ANEOS (Analytic Equation Of State), finding no measurable differences between cavity dimensions in duplicate runs. We applied a simple conductive profile across the ice, with a thermal gradient from surface temperature of 100 K (consistent with European observations [Spencer *et al.*, 1999; Rathbun *et al.*, 2010]) to the appropriate pressure-dependent ice melting temperature at the ice-water contact. Heat flow was calculated according to Bray *et al.* [2014], using a thermal conductivity of $3.3 \text{ W m}^{-1} \text{ K}^{-1}$ [Barr and Showman, 2009]. Damage—a dimensionless parameter describing the degree of fracturing in the target [Collins *et al.*, 2004]—was calculated using an iSALE subroutine based on work of Ivanov *et al.* [1997]. We used a thermal softening parameter [Collins *et al.*, 2004] to account for the effects of temperature increase on the ice yield strength and the block model of acoustic fluidization [Melosh, 1979; Melosh and Ivanov, 1999; Ivanov and Artemieva, 2002] to model impact-related strength degradation and crater collapse. The block model implementation in iSALE assumes that the viscosity of the fluidized zone and the decay time of the fluidization are linearly proportional to impactor radius [Wünnemann and Ivanov, 2003], and we adopted proportionality constants as used in Senft and Stewart [2011] and Bray *et al.* [2014] (Table S1).

Simulated impactors were ice spheres with density 910 kg m^{-3} . Actual cometary impactors would be compositionally heterogeneous and porous, with bulk density about 600 kg m^{-3} [Weissman *et al.*, 2004; A'Hearn *et al.*, 2005]; we used Pi-group gravity scaling [Schmidt and Housen, 1987; Holsapple, 1993] to convert to Europa-appropriate densities and associated bolide sizes. Diameters ranged from 15–8768 m (equivalent to ice bolides 10–6893 m at 26 km s^{-1} or to cometary nuclei 11–8435 m diameter: see Table S2). Resolution tests—duplicate runs at 10 and at 20 cells per projectile radius—showed that the higher resolution made no significant difference in our measurements, so to reduce computation time, we used 10 cells per projectile radius for the bulk of our data collection.

Most simulations were run at 15 km s^{-1} impact velocity, which is less than the estimated 26.5 km s^{-1} median impact velocity at Europa [Zahnle *et al.*, 1998]. High impact velocities require smaller time steps to run smoothly and take far more computation time (adding weeks or months to each simulation), therefore it is a common practice to use 15 km s^{-1} , scaling the energies [Ivanov and Turtle, 2001; Senft and Stewart, 2011; Bray *et al.*, 2014]. We converted the data to equivalent 26.5 km s^{-1} impacts using Pi-group scaling [Schmidt and Housen, 1987; Holsapple, 1993], although it is worth pointing out that the raw 15 km s^{-1} results provide Europa-relevant data, as approximately 8% of JFCs collide with Europa at speeds 9–15 km s^{-1} [Zahnle *et al.*, 1998, Figure 4]. To ensure that the Pi-scaled results were indeed representative of higher-velocity outcomes, we ran some simulations at 26.5 km s^{-1} for comparison. All are reported in Table S2, where it can be verified that both the low-velocity and scaled equivalent impactors at higher velocity produced the same crater geometries.

We varied ice thickness and impact energy to test a wide range of possible scenarios. Europa's ice thickness is unknown: firm constraints are few, and both lateral and secular variation in shell thickness are possible [Nimmo and Manga, 2009]. We therefore simulated impact into a full range of published thickness estimates (1–40 km) [Billings and Kattenhorn, 2005; Nimmo and Manga, 2009]. Impact energies likewise have to be inferred. Jupiter Family Comets (JFCs) probably dominate the impactor population at Europa [Zahnle, 2001], and primary impact craters on Europa record masses of the impactor population in recent geologic time. Midsize (20 km) craters correspond to comets of about 1 km diameter (assuming 600 kg m^{-3} density) [Zahnle *et al.*, 2003], and the largest craters preserved on Europa (≈ 40 –45 km) could have been formed by 1.5–2 km objects [Cox *et al.*, 2008]. As the JFC population includes substantially larger objects [Weissman and Lowry, 2003], and especially because recent analysis suggests an excess of potential

impactors in the 3–6 km range [Fernández *et al.*, 2013], Europa must have experienced larger impacts that are either unrecognized or unpreserved. To accommodate this population, we experimented with Pi-scaled equivalent JFCs as large as 8.5 km diameter.

We recorded transient depth H_t as the maximum depth measured below the preimpact surface. Transient diameter D_t was measured (also using the original ground surface as the datum) at the time when the ejecta curtain ceased expanding and began its return to the surface, which corresponded in the simulations to the appearance of a kink near the base of the ejecta curtain's outer surface (criterion of Gault and Sonett [1982; their Figure 13]). Final depth H_f and diameter D_f were measured relative to the crater rim—which was taken as the topographically highest point of the elevated circum-crater material [e.g., Collins *et al.*, 2002]—after final motions ceased. Cessation of motion was determined by lack of change in depth or diameter over several tens or hundreds of seconds, depending on impact scale. To be sure that we captured final impact crater dimensions, we ran most simulations out to 1500–5000 s postimpact, which was sufficient to confirm final dimensions for most impacts (Table S2).

Impactor recurrence intervals were calculated using cratering rates from Zahnle *et al.* [2003; their Table 3 and Figure 3]. We extracted the estimated occurrence rates for different sized craters (per $10^6 \text{ km}^2 \text{ yr}^{-1}$) from their Figure 3. We used crater scaling to derive the corresponding impactor size and then recast the rates per unit area as recurrence intervals at Europa

3. Results and Discussion

3.1. Comparing Our Outcomes With Existing Scaling Predictions

The relationship between transient and final diameters for icy bodies (based on data from Ganymede and Callisto) [McKinnon and Schenk, 1995] is expected to be within 15% of

$$D_f \approx 1.176D_t^{1.108}$$

A regression through our data (using craters and transitional impacts, for which both D_t and D_f were measurable: Table S2) has $R^2 = 0.993$ and yields the similar relationship

$$D_f \approx 0.872D_t^{1.087}$$

Transitional diameters in our simulations are, on average, within 18% of those predicted by the McKinnon and Schenk relationship, which is comfortably close, especially given the very thin ice used in some of our runs. The degree of agreement is crater size dependent: closer for small craters and less close for larger craters (Figure 1).

The discrepancy between our data and the McKinnon and Schenk [1995] prediction is within expected variance, demonstrating that the simulation outcomes align with independently established scaling laws: this promotes confidence in the results. We propose, however, that the difference between our equation and that of McKinnon and Schenk [1995] may be meaningful and useful in its own right, because of the greater range of crater sizes addressed in our study. The McKinnon and Schenk [1995] relationship is based on craters in the range 5–40 km; those included in this analysis range from 1–145 km, the wider size range probably reduces the uncertainty in the exponent.

3.2. Transient Cavity Geometry Controlled by Ice Thickness and Bolide Size

Transient cavities produced by water impacts differ from those in solid half-spaces [Gault and Sonett, 1982]. Our experiments, which bridge the gap between those end members, reveal how transient cavity geometry evolves as a function of ice thickness and impactor size. As ice becomes thinner relative to bolide diameter, transient cavities become deeper relative to their width (Figure 2). The canonical H_t/D_t ratio for transient cavities in solid half-spaces is in the range 0.25–0.33 [Melosh and Ivanov, 1999], and in this data set, thick-ice impacts—where bolides are shielded from the rheologic effects of the underlying ocean—yield cavities with those kinds of values. As bolides excavate proportionally deeper, however, approaching the ice-water boundary more closely, cavities grow deeper relative to their width. The H_t/D_t ratios for impactors transitional to full penetration are between 0.44 and 0.49, which match those of water impacts [Gault and Sonett, 1982].

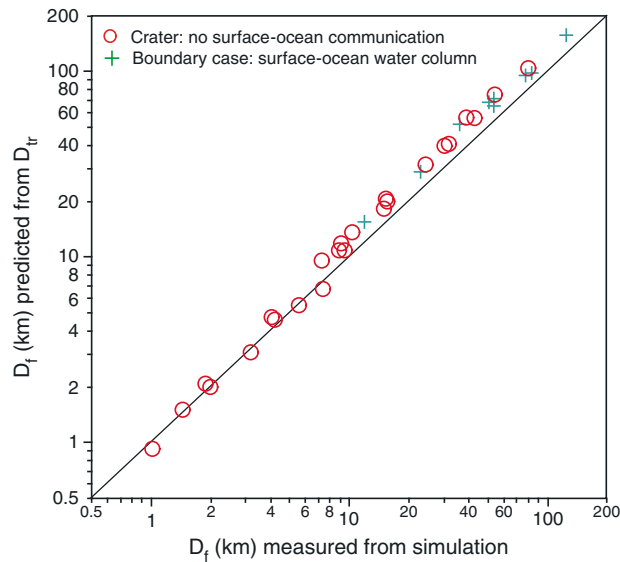


Figure 1. Final crater diameter D_f (measured from simulation data) versus predicted D_f (calculated McKinnon and Schenk [1995] equation). Overall, the agreement between predicted and simulated diameters is very good, with $R^2 > 0.99$. The line on the graph is a simple 1:1 correlation. Smaller craters ($D_f < 10$ km) tend to fall on the 1:1 line; for larger diameters the predicted D_f values are larger than simulated.

3.3. When in the Impact Sequence Does Breaching Occur?

As recognized in previous work [Turtle and Ivanov, 2002; Senft and Stewart, 2011], breaching occurs not during the initial impact stages (compression and excavation) but during crater modification (e.g., Movies S1 and S2). As the target rebounds, a central peak (mostly liquid) rises upward. Additional melting occurs during decompression, and simultaneously the base of the ice crust domes upward. At this point there is (warm) ice separating the liquid in the central peak from the ocean water, but as the peak collapses, the ice-water boundary is still deforming upward. During this stage the last of the ice disappears from the center of the impact structure, either melted or displaced, and there is continuous liquid from surface to underlying ocean. In most cases there is sufficient momentum to generate growth and collapse of one or two more central peaks before the large vertical motions cease.

3.4. The Breaching Criterion: Under What Conditions Is Ice Penetrated?

We simulated nonpenetrating craters, boundary cases where the ice shell was barely breached, and full penetration where impactors punched right through the ice (Table S2). Transient cavity depth H_t (Figure 3) is the primary controlling factor. In nonpenetrating cases, the transient cavity is fully contained in the ice, whereas in full penetrations it extends well down into the underlying water. The geometry of the transient cavity also changes as the ice-thickness: bolide-diameter relationship changes (Figure 2). Of greatest interest are the boundary cases, as those define the limiting conditions for impact penetration. As the ratio between H_t and ice thickness

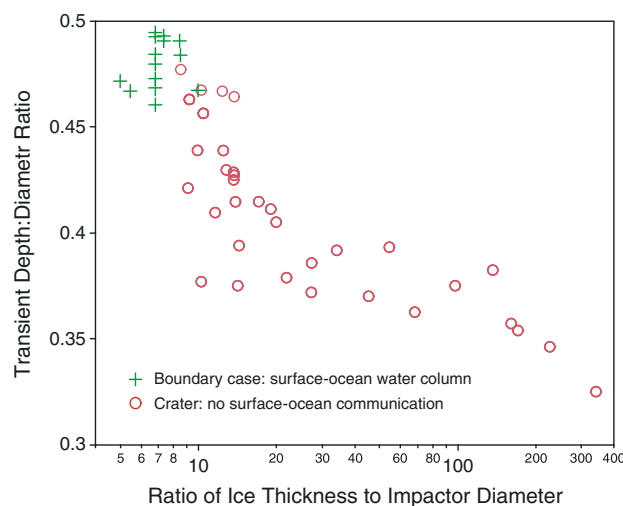


Figure 2. As bolides become bigger relative to ice thickness, transient cavity geometry changes, becoming deeper relative to width.

T_{ice} approaches 1, the transient cavity impinges on the ice-water boundary. The integrity of the ice layer is eventually lost, resulting in a continuous surface-to-ocean water column (Figure 3, Case 2; Movies S1 and S2). This situation is the boundary case for ice breaching (Table S2).

The boundary cases are the lowest-energy occurrence of impact penetration for any ice thickness and can therefore be used to define the conditions at which breaching is inevitable. The boundary cases fall on a straight line in log-log plots of impact parameters (green crosses in Figure 4). In H_t versus T_{ice} space (Figure 4a), a robust regression through these points ($R^2 > 0.99$) defines the breaching equation:

$$H_t(\text{km}) \geq 0.964 T_{ice}(\text{km})^{0.983} \quad (1)$$

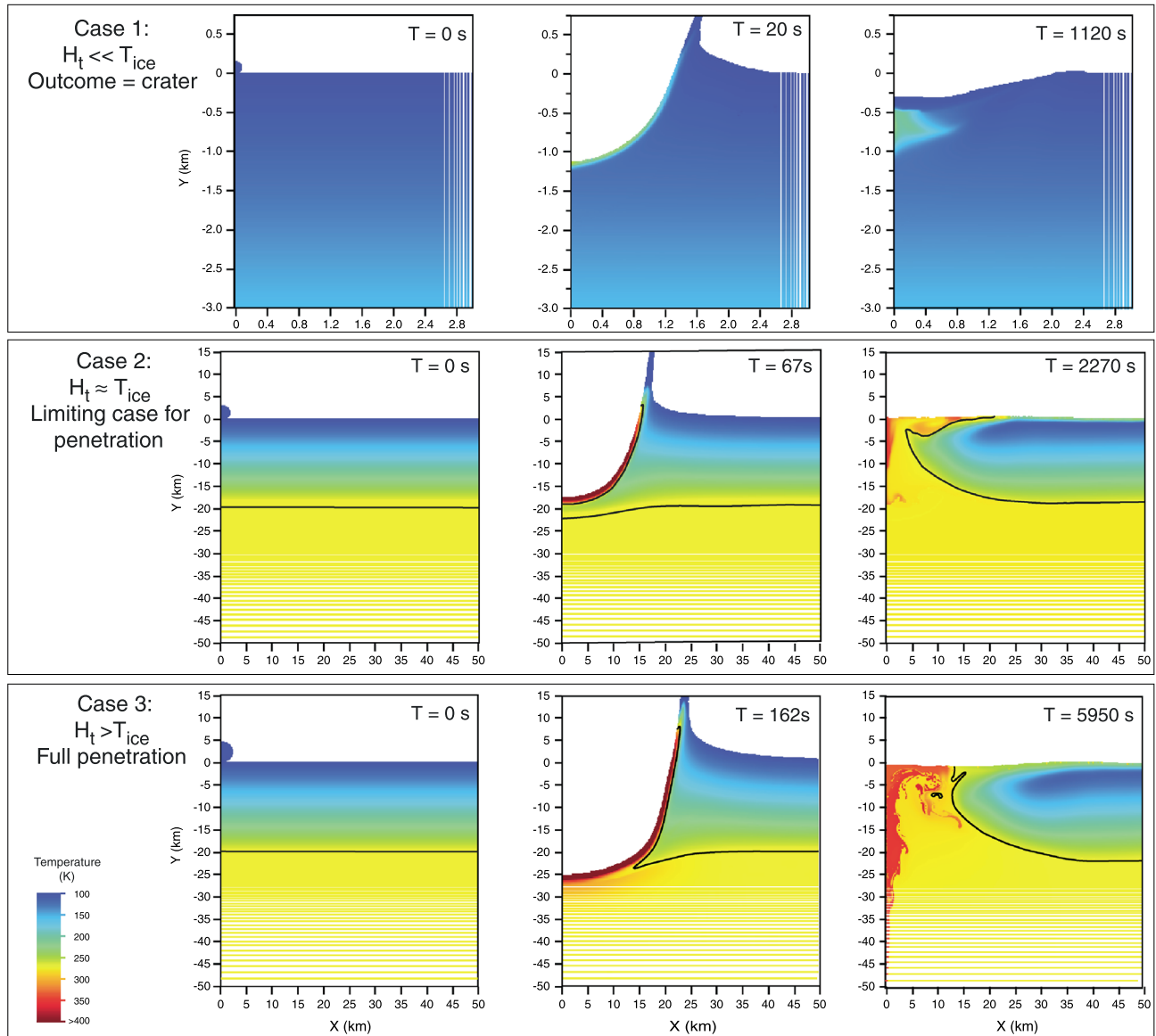


Figure 3. Snapshots for three cases—a nonpenetrating crater, a boundary case breach, and a full penetration—showing initial configuration of impactor and target, the moment of maximum transient cavity depth H_t , and a time late in the crater-modification process. The images show that H_t determines whether an impact will be ice breaching. Targets are color coded for temperature. Time increases from left to right, and each panel shows the postimpact time in seconds. Progressively higher impact energies are arranged from top to bottom. The 273 K isotherms are shown by a thin black line in each case (except Case 1, where the water layer is below the field of view). The three cases shown are run numbers 37.04, 33.11, and 33.23 (see Table S2).

Given the uncertainties inherent in this kind of calculation [McKinnon and Schenk, 1995], it seems reasonable to parse the equation more simply as its approximate equivalent:

$$H_t(\text{km}) \geq 0.9 T_{\text{ice}}(\text{km}) \quad (2)$$

Thus, the breaching criterion is $H_t \approx 0.9 T_{\text{ice}}$.

For a more intuitive comparison, we have also parsed the breaching criterion in terms of impactor diameter D_p (based on an impactor arriving at the median Europa impact velocity of 26.5 km s^{-1} ; Figure 4b, left-hand axis). Penetration occurs when

$$D_p(\text{km}) \geq 0.046 T_{\text{ice}}^{1.283}(\text{km}) \quad (3)$$

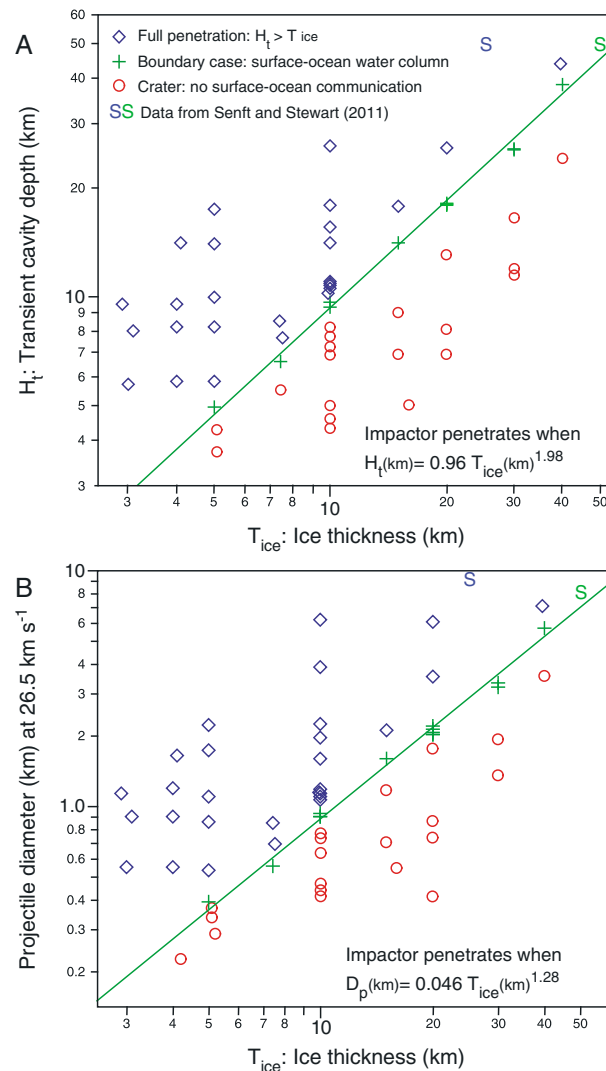


Figure 4. Impact outcomes and breaching criteria. (a) Transient cavity depths in ice of varying thickness. (b) Relationships between impactor size, ice thickness, and impact outcome. Projectile diameters (on the left Y axis in Figure 4) are gravity scaled to represent impacts at the nominal Europa median velocity of 26.5 km s^{-1} . See Table S2 for the data. Points marked with “S” are data from *Senft and Stewart* [2011] and represent impacts (at Ganymede). The blue S represents full breach of a 25 km ice crust, equivalent to our full-penetration outcomes; the green S represents the case where the transient cavity extends to the base of a 50 km ice crust, equivalent to our boundary case data. Regression lines ($R^2 > 0.99$) are fit to the boundary case outcomes (green crosses), which represent the lowest energy and/or smallest ice thickness at which full ice penetration is achieved. The equations of these lines provide breaching criteria for impacts at Europa.

geologic time. Determining the frequency with which this has happened then becomes a question of narrowing the likely thickness range.

3.5. Constraints on European Ice Thickness

Schenk's [2002] classic depth-diameter (H/D) curve for European craters shows that small features follow the same trend as craters on rocky bodies, but that at diameters $> 8 \text{ km}$, the H/D curve flattens and then rolls over sharply, with larger craters becoming dramatically shallower as size increases (Figure 5). Numerical

We tested our results by incorporating data from other studies into this analytical framework. Figure 4 includes two data points from *Senft and Stewart* [2011], representing impact at Ganymede: a 10 km bolide hitting 25 km ice had $H_t > T_{ice}$, and thus corresponds to a full penetration (blue S on Figure 4); the same impactor into 50 km ice had $H_t \approx T_{ice}$ and is therefore plotted as a boundary case (green S on Figure 4). The boundary case impact is colinear with our data, validating the breaching criteria given above.

A second test, and additional insight into impact dynamics, comes from comparison of the data with those of *Bray et al.* [2014], who reported that full penetration ($H_t > T_{ice}$) occurred where T_{ice} was less than 7 times D_p (for ice projectiles at 15 km s^{-1}). We confirm this result (validating our methods) but show further that it applies only to ice thicknesses in the range 10–30 km and that in fact the relationship varies systematically with ice thickness: for thinner ice, the projectile-diameter multiplier increases (to about 9 in 5 km ice), and it decreases for thicker ice (5 in 40 km ice). Further comparison with the *Senft and Stewart* [2011] simulations—in which the boundary case penetration occurred when T_{ice} was 5 times greater than D_p (Figure 4)—underscores this interpretation.

These results (Table S2) mean that ice 5 km thick would be breached by cometary impactors 400–500 m diameter; that 10 km ice would be breached by an object $\approx 1 \text{ km}$ across; and that even 40 km ice would be subject to penetration by a bolide of 5–7 km diameter (depending on density and impact velocity). Impactors of these sizes are expected to encounter Europa at intervals ranging from $< 100 \text{ kyr}$ to 250 Ma (based on *Zahnle et al.* [2003]), which means that whether Europa's ice is thick or thin, it has been subject to penetration over

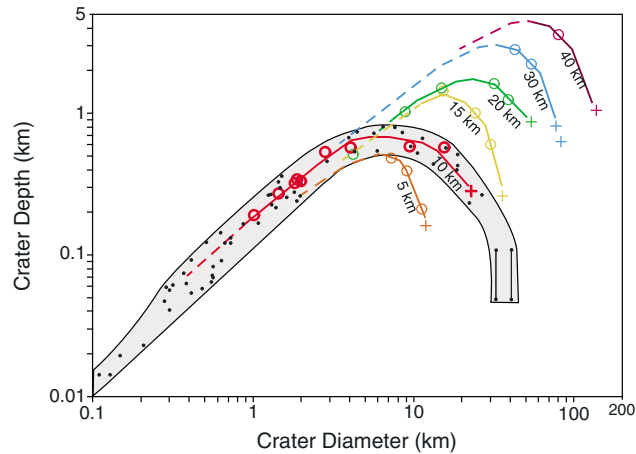


Figure 5. Depth-diameter measurements from Europa [Schenk, 2002] and shock physics code simulations (Table S2). European values are shown as black dots; the enclosing grey envelope shows the likely range of values for Europa. Simulated craters are open circles; boundary case penetrations are crosses, color coded for crust thickness. (Full penetration impacts are not plotted because crater-center oscillations continue beyond the run time, precluding accurate measurements [Senft and Stewart, 2011]). Lines connecting simulation data points represent depth-diameter trends for different ice thicknesses (solid where constrained by data, dashed where inferred). The characteristic rollover occurs at small crater diameters in thinner crust and at progressively larger diameters as crust gets thicker [Bray et al., 2014]. The data for the 10 km thick crust fall entirely within the envelope containing the European measurements, suggesting that 10 km may be a good estimate for ice thickness at Europa.

point is that multiple studies converge on ice thickness estimates in the vicinity of 10 km. Our calculations and those of Bray et al. [2014] also align with Hand and Chyba's [2007] 4–15 km value from analysis of Galileo magnetometer data, and the median of published ice thickness estimates for Europa [Billings and Kattenhorn, 2005] is 13 km. We do not imply that our model provides an absolutely correct answer (see note about ice physics above, plus the probability that there are lateral thickness variations [Nimmo and Manga, 2009]), but we do believe that 10 km represents a good working estimate for a characteristic European ice shell thickness.

3.6. Combining Simulation Results With European Crater Geomorphology

Europa's larger (>10 km diameter) craters fall into three categories, with increasing levels of geomorphologic oddness: normal complex (e.g., Maeve, Cilix, and Govannan), disrupted central peak (Amergin, Manannán, and Pwyll), and multiring basin (Tyre and Callanish) [Schenk and Turtle, 2009]. All plot on the descending limb of the Schenk [2002] rollover curve (Figure 5), indicating increased interaction with the underlying water and possible transition to penetration [Kadel et al., 2000; Moore et al., 2001; Schenk, 2002; Bierhaus et al., 2009; Pappalardo, 2010].

Comparison of real craters with the simulation data provides interpretive insights. Figure 4a shows simulated final crater diameter D_f as a function of T_{ice} . In this parameter space, the breaching criterion (again based on regression through the boundary cases) is

$$D_f = 1.75 T_{ice}^{1.14} \quad (4)$$

The grey band surrounding the boundary case data points is our interpretation of the likely transition zone. It is based on 95% confidence bounds on the regression line but drawn a bit fatter to acknowledge imprecision of the interpretation: pending better characterization of the rheology of Europa's crust, we cannot be too bullish about the exact location of the line.

This framework provides a backhand, semiquantitative way to think about crust thickness variations, using the diameters of mapped craters on Europa. The crater diameters are known. The ice thickness is not. But the slope of the breaching line in Figure 6 places limitations on possible ice thicknesses at the time and place

simulations duplicating European H/D trends can therefore provide insight into European ice thickness [Bray et al., 2014].

Simulated impacts produce the same rollover pattern at all ice thicknesses but only for ≈ 10 km ice do the data fall on the Schenk curve (Figure 5). This result is slightly different from that of Bray et al. [2014], for whom impacts into 7 km thick ice fell within the Schenk envelope. The discrepancy can be attributed to a small difference in constitutive model inputs (we used a value of zero for the cohesion of fully damaged ice [Ivanov et al., 1997; Senft and Stewart, 2011], whereas Bray et al. used 0.05 MPa). Given the limitations in our understanding of impact physics in low-temperature ice, the discrepancy between these two estimates of European ice thickness serves as a useful measure of uncertainty. The key

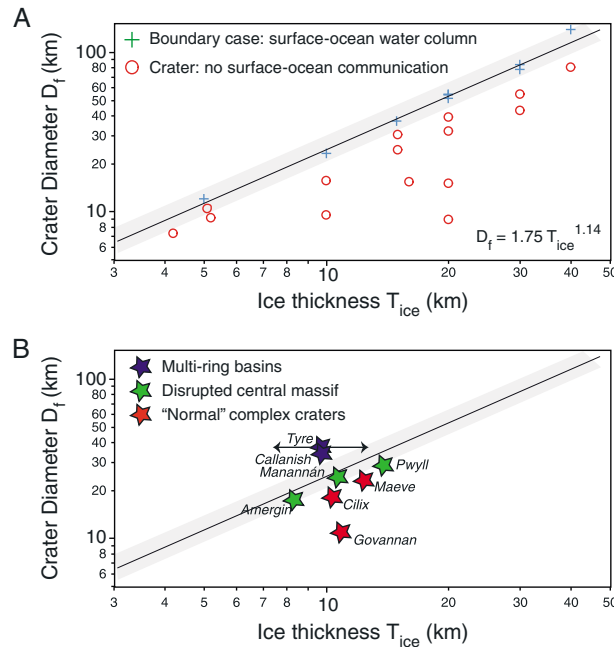


Figure 6. Final crater diameter D_f versus ice thickness T_{ice} . (a) Model data are shown. The line of fit ($R^2 = 0.989$) is run through the boundary cases (green crosses) and defines another version of the breaching criterion:

$$D_f \geq 1.75 T_{ice}^{1.14}$$

The pale grey band surrounding the regression line is a qualitative assessment of the transition zone width, acknowledging the unquantifiable but real uncertainties in the data: for a given ice thickness, the transition from crater to penetration is expected to happen somewhere in this region. (b) Europa's craters (diameters from [Schenk and Turtle, 2009]) in relation to this transition zone. Diameters for the multiring basins and the transitional/disrupted craters (except Pwyll) are not precisely known [Schenk and Turtle, 2009], so the stars are deliberately large, to encompass all likely diameters. Double-headed arrows represent possible ice thicknesses consistent with crater geomorphology and model predictions.

the base of the transition zone (Figure 6b), in which case again the slope of the breaching line provides some constraint on ice thickness. By this interpretation, ice in the Amerrgin region (8–9 km) is or was thinner than that near Pwyll (12–13 km). As pointed out by Schenk and Turtle [2009], the morphological differences between the similarly sized Maeve (normal complex) and Manannán (disrupted central peak) suggest different crust thicknesses at their formation sites, and that is supported by this analysis: for Manannán to plot at the base of the transition zone and for Maeve to plot below it requires that Manannán formed in thinner crust.

The multiring basins Callanish and Tyre are interpreted to represent penetration to the underlying ocean [Kadel et al., 2000; Moore et al., 2001; Pappalardo, 2010], so should plot above the breaching line; but as there is no evidence for wide-scale crust disruption of the sort that is expected to occur from a full-on ice breach [Croft, 1981; Ong et al., 2005; Cox et al., 2008], they are probably close to the boundary (Figure 6b). To plot above the breaching line, these basins must have formed in ice thinner than ≈ 15 km.

Thus, interpretation of European crater geomorphology dovetails with the results from the numerical simulations. Their measured diameters, juxtaposed with the calculated breaching criterion, produce ice thickness estimates in the range 8–15 km, which (given all the inherent uncertainties) is fully consistent with the thickness predicted from the simulations.

that the craters formed. For example, normal complex craters must plot below the breaching line (Figure 6b), as the simulated craters do in Figure 6a. Smaller craters like Govannan are not useful in this analysis because they fall well below the breaching line and could have formed in a wide range of ice thicknesses. But larger craters provide tighter constraints because there is a limited parameter space beneath the breaching line in which they can be plotted; thus, the range of possible ice thicknesses is restricted. From this we can infer that Cilix could not have formed in ice less than about 9 km thick, and Maeve requires at least 11 km ice (Figure 6b).

The next size class, disrupted central-massif craters, exhibits a strange geomorphology related somehow to ice thickness and rheology [Schenk and Turtle, 2009]. The three known craters in this category (Manannán, Amerrgin, and Pwyll) have shallow floors, lumpy, chaos-like fill, and off-center disorganized internal massifs, with vestigial and/or discontinuous rims [Moore et al., 2001; Schenk and Turtle, 2009]. Although Manannán required brittle ice for formation, that layer may have extended only to the transient crater depth, i.e., the impactor might have penetrated to a mobile layer beneath [Moore et al., 2001; Greenberg and Geissler, 2002]. Recognizing that we do not fully understand them, we propose that these features should plot somewhere at or near

4. Ice-Breaching Frequency and Europa's Missing Large-Crater Population

If Callanish and Tyre preserve boundary case ($H_t \approx 0.9T_{ice}$) impact sites, and if those 40–50 km features represent cometary impactors in the range 2–2.5 km diameter [Zahnle *et al.*, 2003], then the recurrence interval for penetrating impactors at Europa (based on relationships in Zahnle *et al.* [2003]) is surprisingly short: between 7 and 11 Ma. Obviously, full penetrators ($H_t > T_{ice}$) are less frequent than this but not by much, and the 40–90 Ma crater retention age [Bierhaus *et al.*, 2009] means that some scars of larger penetrating impacts should be preserved on Europa's surface.

That there is a “missing” population of larger craters on Europa is not a new observation: studies of impact frequency [Zahnle *et al.*, 2008] and crater populations [Bierhaus *et al.*, 2009] predict that Europa should have several craters larger than 50 km. Given that the largest recognized craters on Europa (Tyre and Callanish) are likely to have penetrated, if marginally, to the underlying ocean [Kadel *et al.*, 2000; Moore *et al.*, 2001; Pappalardo, 2010], and given also that the data (Table S2) indicate that impacts producing craters 50 km diameter or larger on Europa would have $H_t > T_{ice}$, it seems likely that the missing crater population may be represented by a category of fully penetrating impacts, with geomorphology that has not yet been recognized [Cox *et al.*, 2008; Bierhaus *et al.*, 2009].

4.1. Chaos Terrain May Mark the Penetrating Impact Sites

A combination of observations suggests that chaos terrain may preserve the signature of penetrating impacts. Supporting evidence includes geomorphic similarities between European chaos and terrestrial ice-explosion experiments [Billings and Kattenhorn, 2003; Billings, 2004]; impact experiments at both low and hypervelocity that duplicate the features of chaos terrain [Ong *et al.*, 2004; Scheider, 2007; Scheider and Cox, 2007]; analysis of size-frequency distribution of chaos areas and craters, which matches a Europa-appropriate production function [Cox *et al.*, 2008]; and the size-area distribution of secondary craters around the large chaos area Thera Macula, which shows a radial, logarithmic size decrease away from Thera [Cox *et al.*, 2008]. Separately, but even more strongly in combination, these observations support the hypothesis that some chaos terrain may mark sites of penetrating impacts. We must therefore look on more closely at Europa for the missing penetrating impact sites.

5. Relevance for Astrobiology: Impact-Mediated Transfer Between Surface and Ocean

Conservative estimates suggest 1–10 Gt of comet-borne C (in addition to N, P, and S) has been deposited at Europa during solar system history [Pierazzo and Chyba, 2002]. Prebiotic compounds, as well as spores and bacteria, can survive impact shock pressures [Burchell *et al.*, 2004], and although the lifetime of organic molecules at Europa's surface is very brief [Varnes and Jakosky, 1999], they may be buried and shielded by impact gardening. Regolith formation and tidal-tectonic crustal movements may convey organic materials, as well as the energy-bearing products of irradiation, downward within the ice [Cooper *et al.*, 2001; Greenberg, 2010]. Transfer of these materials to the underlying ocean is a key aspect of astrobiologic models [e.g., Chyba and Phillips, 2001; Hand *et al.*, 2009].

Penetrating impacts play into this in three ways: by direct delivery of organic material to the ocean, by opening a surface-to-ocean conduit through which materials (chemical-energy-bearing radiation products as well as immigrant organic matter) can fall, and by generating turbulent mixing through most of the water column (e.g., Figure 3, Case 3, $T = 5950$ s).

Direct ocean seeding by the impactor is unlikely. Because low-density porous impactors—such as the JFCs that constitute the main impactor population at Europa [Zahnle *et al.*, 2003]—are subject to wholesale vaporization, with most of the mass being driven outward in the expansion plume [Pierazzo and Chyba, 2002], surviving prebiotic payload from comets is unlikely to end up in the crater. But there are other paths to the subsurface. Organic freight deposited at distance from the impact site might enter the ocean directly if it chances to land on an unfrozen conduit created by a prior impact, but this is probably a rare event. It is more likely to be incorporated into regolith and buried by later ejecta, for potential transfer to the subsurface ocean by tectonic process or by subsequent impact. It is this latter case that we consider the most likely mechanism for surface-to-ocean transport of both organic deposits and radiolytic oxidants.

Impact-related erosion of pre-existing materials during a penetrating impact event seems a likely way for prebiotic materials to enter the ocean. Creation of a surface-to-ocean conduit means that organic and radiolytic material warehoused within the ice crust can be integrated during and after the impact event, as fragmented and melted ice mix with exposed water. In broad thought-experiment terms, there are three main ways this could happen. The most obvious is that collapsing crater walls will shed block ice into the open hole post impact. Such ice will be fragmented by collisions with other clasts, increasing the exposed surface area. At the same time, the boiling mass of exposed water in the throat of the impact site will be an effective melting agent, acting on all surfaces with which it comes in contact (crater walls and fallen blocks). In addition, seiches set up in the impact goblet will overtop the crater walls as tsunami-like bores (Movies S3 and S4), eroding material as they surge across Europa's surface (both by scour at the base of the turbulent flow and by dissolution of surface materials by the liquid water). Some of this (salt-bearing) water will pond and freeze on the surface, but much will flow back, either overland or—by analogy with glacial hydrology, e.g., [Benn *et al.*, 2009]—through cracks or possibly even moulin-like ducts. The return flow will carry with it prebiotic materials, probably including organic compounds deposited by previous impactors.

6. Summary and Conclusions

Detection of salts in surface ice indicates communication between Europa's ocean and the exterior [Brown and Hand, 2013; Hand and Carlson, 2015], and simulations demonstrate that the body's ice is vulnerable to penetration by impact. We do not claim that impact is the only mechanism by which surface-to-ocean communication can occur, but impact penetration provides a viable mechanism for large-scale mass transfer, by which oceanic salts could arrive at the surface and by which prebiotic materials could be transported to the ocean.

Simulations indicate that events producing transient craters with depth >90% of the ice thickness are sufficient to result in full surface-to-ocean conduits. Although the absolute rate at which such events occur depends on European ice thickness, which is not fully constrained, the breaching recurrence interval for likely ice thicknesses (7–13 km) might be less than 10 Ma. Even if ice is thicker than this, breaching is still indicated at timescales that are geologically quite short (>250 Ma for breaching of 40 km ice). It therefore seems inescapable that Europa's ice has been breached by impact. The challenge now is to recognize the sites where it has happened: chaos terrain may hold the key.

Acknowledgments

Data reported in this paper are tabulated in the supporting information. Additional materials such as detailed run outputs or movies are available on request from the corresponding author. We gratefully acknowledge the developers of iSALE: without the work they put into the code, none of this would have been possible. We are grateful also to Jay Melosh and Robert Weiss for their early discussions and advice on this project and to Gareth Collins, Veronica Bray, and an anonymous reviewer, whose thoughtful commentary improved the paper. This work was supported by the Sperry Family Fund for Geosciences.

References

- A'Hearn, M. F., et al. (2005), Deep impact: Excavating comet Tempel 1, *Science*, 310(5746), 258–264, doi:10.1126/science.1118923.
- Amdsen, A. A., H. M. Ruppel, and C. W. Hirt (1980), SALE: Simplified ALE computer program for fluid flow at all speeds, 106 pp., Los Alamos, New Mexico.
- Barr, A. C., and A. P. Showman (2009), Heat transfer in Europa's icy shell, in *Europa*, edited by R. T. Pappalardo, W. B. McKinnon, and K. K. Khurana, pp. 405–430, Univ. of Ariz. Press, Tucson.
- Benn, D., J. Gulley, A. Luckman, A. Adamek, and P. S. Glowacki (2009), Englacial drainage systems formed by hydrologically driven crevasse propagation, *J. Glaciol.*, 55(191), 513–523.
- Bierhaus, E. B., K. Zahnle, and C. R. Chapman (2009), Europa's crater distributions and surface ages, in *Europa*, edited by R. T. Pappalardo, W. B. McKinnon, and K. K. Khurana, pp. 161–180, Univ. of Ariz. Press, Tucson.
- Billings, S. E. (2004), Analysis of the ice shell of Jupiter's moon, Europa: Estimation of ice thickness and an examination of impact effects into a floating ice shell, MS thesis, 113 pp., Univ. of Idaho, Moscow.
- Billings, S. E., and S. A. Kattenhorn (2003), Comparison between terrestrial explosion crater morphology in floating ice and European chaos, Lunar and Planetary Science XXXIV, Abstract 1955.
- Billings, S. E., and S. A. Kattenhorn (2005), The great thickness debate: Ice shell thickness models for Europa and comparisons with estimates based on flexure at ridges, *Icarus*, 177, 397–412, doi:10.1016/j.icarus.2005.03.013.
- Bray, V. J., G. S. Collins, J. V. Morgan, and P. M. Schenk (2008), The effect of target properties on crater morphology: Comparison of central peak craters on the Moon and Ganymede, *Meteorit. Planet. Sci.*, 43, 1979–1992.
- Bray, V. J., G. S. Collins, J. V. Morgan, H. J. Melosh, and P. M. Schenk (2014), Hydrocode simulation of Ganymede and Europa cratering trends—How thick is Europa's crust?, *Icarus*, 231, 394–406, doi:10.1016/j.icarus.2013.12.009.
- Brown, M. E., and K. P. Hand (2013), Salts and radiation products on the surface of Europa, *Astron. J.*, 145(4), 110. [Available at <http://stacks.iop.org/1538-3881/145/i=4/a=110>.]
- Burchell, M. J., J. R. Mann, and A. W. Bunch (2004), Survival of bacteria and spores under extreme shock pressures, *Mon. Not. R. Astron. Soc.*, 352, 1273–1278.
- Chyba, C. F., and C. B. Phillips (2001), Possible ecosystems and the search for life on Europa, *Proc. Natl. Acad. Sci.*, 98, 801–804.
- Collins, G. S., H. J. Melosh, J. V. Morgan, and M. R. Warner (2002), Hydrocode simulations of Chicxulub crater collapse and peak-ring formation, *Icarus*, 157(1), 24–33.
- Collins, G. S., H. J. Melosh, and B. A. Ivanov (2004), Modeling damage and deformation in impact situations, *Meteorit. Planet. Sci.*, 39, 217–231.
- Collins, G. S., H. J. Melosh, and K. Wünnemann (2011), Improvements to the ϵ - α porous compaction model for simulating impacts into high-porosity solar system objects, *Int. J. Impact Eng.*, 38, 434–439, doi:10.1016/j.ijimpeng.2010.10.013.

- Cooper, J. F., R. E. Johnson, B. H. Mauk, H. B. Garrett, and N. Gehrels (2001), Energetic ion and electron irradiation of the icy Galilean satellites, *Icarus*, *149*, 133–159.
- Cox, R., L. C. F. Ong, M. Arakawa, and K. C. Scheider (2008), Impact penetration of Europa's ice crust as a mechanism for formation of chaos terrain, *Meteorit. Planet. Sci.*, *43*, 2027–2048.
- Croft, S. K. (1981), Hypervelocity impact craters in icy media. *Lunar and Planetary Science XII*, pp. 190–192.
- Fernández, Y. R., et al. (2013), Thermal properties, sizes, and size distribution of Jupiter-family cometary nuclei, *Icarus*, *226*(1), 1138–1170, doi:10.1016/j.icarus.2013.07.021.
- Gault, D. E., and C. P. Sonett (1982), Laboratory simulation of pelagic asteroidal impact: Atmospheric injection, benthic topography, and the surface wave radiation field, in *Geological Implications of Impacts of Large Asteroids and Comets on the Earth*, *Geol. Soc. Am. Spec. Pap.*, vol. 190, edited by L. T. Silver and P. H. Schultz, pp. 69–92, Geol. Soc. Am., Boulder, Colo.
- Greenberg, R. (2010), Transport rates of radiolytic substances into Europa's ocean: Implications for the potential origin and maintenance of life, *Astrobiology*, *10*, 275–283, doi:10.1089/ast.2009.0386.
- Greenberg, R., and P. Geissler (2002), Europa's dynamic icy crust, *Meteorit. Planet. Sci.*, *37*, 1685–1710.
- Hand, K. P., and R. W. Carlson (2015), Europa's surface color suggests an ocean rich with sodium chloride, *Geophys. Res. Lett.*, *42*, 3174–3178, doi:10.1002/2015GL063559.
- Hand, K. P., and C. F. Chyba (2007), Empirical constraints on the salinity of the European ocean and implications for a thin ice shell, *Icarus*, *189*, 424–438.
- Hand, K. P., C. F. Chyba, J. C. Priscu, R. W. Carlson, and K. H. Nealson (2009), Astrobiology and the potential for life on Europa, in *Europa*, edited by R. T. Pappalardo, W. B. McKinnon, and K. K. Khurana, pp. 589–629, Univ. of Ariz. Press, Tucson.
- Holsapple, K. A. (1993), The scaling of impact processes in planetary sciences, *Annu. Rev. Earth Planet. Sci.*, *21*, 333–373.
- Ivanov, B. A., and N. A. Artemieva (2002), Numerical modeling of the formation of large impact craters, *Geol. Soc. Am. Spec. Pap.*, *356*, 619–630.
- Ivanov, B. A., and E. P. Turtle (2001), Penetration of the ice crust on Europa during impact cratering: A lower limit for ice thickness, 4th Lunar and Planetary Laboratory Conference, Abstract 1013.
- Ivanov, B. A., D. Deniem, and G. Neukum (1997), Implementation of dynamic strength models into 2D hydrocodes: Applications for atmospheric breakup and impact cratering, *Int. J. Impact Eng.*, *20*, 411–430.
- Jutzi, M., K. A. Holsapple, K. Wünnemann, and P. Michel (2015), Modeling asteroid collisions and impact processes, in *Asteroids IV*, edited by P. Michel, F. E. DeMeo, and W. F. Bottke, Univ. of Ariz. Press, Tucson, arXiv:1502.01844 [astro-ph.EP].
- Kadel, S. D., F. C. Chuang, R. Greeley, J. M. Moore, and G. S. Team (2000), Geological history of the Tyre region of Europa: A regional perspective on European surface features and ice thickness, *J. Geophys. Res.*, *105*, 22,657–22,669, doi:10.1029/1999JE001203.
- Kivelson, M. C., K. K. Khurana, C. T. Russell, M. Volwerk, R. J. Walker, and C. Zimmer (2000), Galileo magnetometer measurements: A stronger case for a subsurface ocean at Europa, *Science*, *289*, 1340–1343.
- McKinnon, W. B., and P. Schenk (1995), Estimates of comet fragment masses from impact crater chains on Callisto and Ganymede, *Geophys. Res. Lett.*, *22*, 1829–1832, doi:10.1029/95GL01422.
- Melosh, H. J. (1979), Acoustic fluidization: A new geologic process?, *J. Geophys. Res.*, *84*, 7513–7520, doi:10.1029/JB084iB13p07513.
- Melosh, H. J., and B. A. Ivanov (1999), Impact crater collapse, *Annu. Rev. Earth Planet. Sci.*, *27*, 385–415.
- Moore, J. M., et al. (2001), Impact features on Europa: Results of the Galileo Europa Mission (GEM), *Icarus*, *151*, 93–111.
- Nimmo, F., and B. Giese (2005), Thermal and topographic tests of Europa chaos formation from Galileo E15 observations, *Icarus*, *177*, 327–340, doi:10.1016/j.icarus.2004.10.034.
- Nimmo, F., and M. Manga (2009), Geodynamics of Europa's icy shell, in *Europa*, edited by R. T. Pappalardo, W. B. McKinnon, and K. K. Khurana, pp. 381–404, Univ. of Ariz. Press, Tucson.
- Ong, L. C. F., R. Cox, and M. Arakawa (2004), Craters and chaos structures on Europa, *Japanese Society for Planetary Sciences Annual Meeting Abstracts*, *7*.
- Ong, L. C. F., G. Gisler, R. Weaver, and M. Gittings (2005), Numerical simulations of impactor penetration into ice-over-water targets, paper presented at Lunar and Planetary Science XXXVI, Abstract 2400, Lunar and Planetary Institute, Houston, Tex.
- Pappalardo, R. T. (2010), Seeking Europa's ocean, in *Galileo's Medicean Moons: Their Impact on 400 Years of Discovery*, *Proc. IAU Symp.*, vol. 269, edited by C. Barbieri et al., pp. 101–114, Cambridge Univ. Press, Cambridge, U. K.
- Pierazzo, E., and C. F. Chyba (2002), Cometary delivery of biogenic elements to Europa, *Icarus*, *157*, 120–127.
- Pierazzo, E., et al. (2008), Validation of numerical codes for impact and explosion cratering: Impacts on strengthless and metal targets, *Meteorit. Planet. Sci.*, *43*, 1917–1938.
- Rathbun, J. A., N. J. Rodriguez, and J. R. Spencer (2010), Galileo PPR observations of Europa: Hotspot detection limits and surface thermal properties, *Icarus*, *210*, 763–769, doi:10.1016/j.icarus.2010.07.017.
- Scheider, K. C. (2007), Impact processes on Jupiter's moon, Europa, B.A. thesis, 120 pp., Williams College, Williamstown, Mass.
- Scheider, K. C., and R. Cox (2007), Ice penetrating impacts: Insights from hypervelocity impact experiments and Galileo image mapping of Europa, paper presented at Bridging the Gap II: Effects of Target Processes on the Impact Cratering Process: LPI Abstract 8034.
- Schenk, P., and E. P. Turtle (2009), Europa's impact craters: Probes of the icy shell, in *Europa*, edited by R. T. Pappalardo, W. B. McKinnon, and K. K. Khurana, pp. 181–198, Univ. of Ariz. Press, Tucson.
- Schenk, P. M. (2002), Thickness constraints on the icy shells of the Galilean satellites from a comparison of crater shapes, *Nature*, *417*, 419–421.
- Schmidt, R. M., and K. R. Housen (1987), Some recent advances in the scaling of impact and explosion cratering, *Int. J. Impact Eng.*, *5*(1), 543–560.
- Senft, L. E., and S. T. Stewart (2011), Modeling the morphological diversity of impact craters on icy satellites, *Icarus*, *214*, 67–81, doi:10.1016/j.icarus.2011.04.015.
- Singer, K. N., W. B. McKinnon, and P. M. Schenk (2010), Pits, spots, uplifts, and small chaos regions on Europa: Evidence for diapiric upwelling from morphology and morphometry, *41st Lunar and Planetary Science Conference*, Abstract 2195.
- Spencer, J. R., L. K. Tamppari, T. Z. Martin, and L. D. Travis (1999), Temperatures on Europa from Galileo PPR: Nighttime thermal anomalies, *Science*, *284*, 1514–1516, doi:10.1126/science.284.5419.1514.
- Turtle, E. P., and B. A. Ivanov (2002), Numerical simulations of impact crater excavation and collapse on Europa: Implications for ice thickness, *Lunar and Planetary Science XXXIII*, Abstract 1431.
- Turtle, E. P., and E. Pierazzo (2001), Thickness of a European ice shell from impact crater simulations, *Science*, *294*, 1326–1328.
- Varnes, E. S., and B. M. Jakosky (1999), Lifetime of organic molecules at the surface of Europa, *Abstracts of the Lunar and Planetary Science Conference*, *30*, contribution no. 1082.
- Weiss, R., K. Wünnemann, and H. Bahlburg (2006), Numerical modelling of generation, propagation and run-up of tsunamis caused by oceanic impacts: Model strategy and technical solutions, *Geophys. J. Int.*, *167*, 77–88, doi:10.1111/j.1365-246X.2006.02889.x.

- Weissman, P. R., and S. C. Lowry (2003), The size distribution of Jupiter-family cometary nuclei, paper presented at Lunar and Planetary Science XXXIV, Abstract 2003, Lunar and Planetary Institute, Houston, Tex.
- Weissman, P. R., E. Asphaug, and S. C. Lowry (2004), Structure and density of cometary nuclei, in *Comets II*, edited by M. Festou, H. U. Keller, and H. A. Weaver, pp. 337–357, Univ. of Ariz. Press, Tucson.
- Wünnemann, K., and B. A. Ivanov (2003), Numerical modelling of the impact crater depth-diameter dependence in an acoustically fluidized target, *Planet. Space Sci.*, *51*, 831–845.
- Wünnemann, K., G. S. Collins, and H. J. Melosh (2006), A strain-based porosity model for use in hydrocode simulations of impacts and implications for transient crater growth in porous targets, *Icarus*, *180*, 514–527, doi:10.1016/j.icarus.2005.10.013.
- Zahnle, K. (2001), Cratering rates on Europa, Lunar and Planetary Science XXXII, Abstract 1699.
- Zahnle, K., L. Dones, and H. Levison (1998), Cratering rates on the Galilean satellites, *Icarus*, *136*, 202–222.
- Zahnle, K., P. Schenk, H. Levison, and L. Dones (2003), Cratering rates in the outer Solar System, *Icarus*, *163*, 263–289.
- Zahnle, K., J. L. Alvarillos, A. Dobrovolskis, and P. Hamill (2008), Secondary and sesquinary craters on Europa, *Icarus*, *194*, 660–674, doi:10.1016/j.icarus.2007.10.024.